

1 Article

2 Hydrophilic silver nanoparticles loaded into niosomes: 3 physical-chemical characterization in view of biological applications

4

5 Federica Rinaldi¹, Elena del Favero², Johannes Moeller³, Patrizia Nadia Hanieh⁴ Daniele Passeri⁵,

6 Marco Rossi⁵, Livia Angeloni⁵, Iole Venditti^{6*}, Carlotta Marianecchi^{6*}, Maria Carafa^{7**}, Ilaria

7 Fratoddi^{7**}

8

9 ¹ Center for Life Nano Science@Sapienza, Istituto Italiano di Tecnologia (ITT), Rome, Italy;
10 federica.rinaldi@iit.it;

11 ² Department of Medical Biotechnology and Translational Medicine, University of Milan, [V.le F. III](#)
12 [Cervi 93, 20090 Segrate](#), Italy; elena.delfavero@unimi.it.

13 ³ European XFEL GmbH Holzkoppel 4, 22869 Schenefeld Germany;

14 ⁴ Department of Drug Chemistry and Technologies, Sapienza University, Rome, Italy;

15 patrizianadia.hanieh@uniroma1.it; carlotta.marianecchi@uniroma1.it; maria.carafa@uniroma1.it

16 ⁵ Department of Basic and Applied Sciences for Engineering, Sapienza University of Rome, Via A.

17 Scarpa 14, 00161 Rome, Italy; daniele.passeri@uniroma1.it; marco.rossi@uniroma1.it.

18 ⁶ Department of Sciences, Roma Tre University, Rome Italy; iole.venditti@uniroma3.it

19 ⁷ Department of Chemistry, Sapienza University, Rome, Italy; ilaria.fratoddi@uniroma1.it

20
21 * Correspondence: iole.venditti@uniroma3.it; Tel.: +39-06-57333388;

22 carlotta.marianecchi@uniroma1.it; Tel.: +39-06-49913970

Formattato: Non Evidenziato

23 **co-last authors

24 Received: date; Accepted: date; Published: date

25
26 Suggested referee

27 1. x

28 [2.* Anna Fadda, Dipartimento di Scienze della Vita e dell'Ambiente, via Ospedale, 72,](#)
29 [09124 Cagliari, 070 675 8565, fax 070 675 8710, e-mail mfadda@unica.it](#)

Formattato: Tipo di carattere: 12 pt

30
31 [3.Cesar Viseras, Facultad de Farmacia, Departamento de Farmacia y Tecnología](#)
32 [Farmacéutica](#)

Formattato: Tipo di carattere: Times New Roman, 12 pt

33 [Campus Universitario de Cartuja C.P. 18071 \(Granada\) Granada, e-mail: \[cviseras@ugr.es\]\(mailto:cviseras@ugr.es\)](#)

Formattato: Tipo di carattere: Times New Roman, 12 pt

34 *

Formattato: Tipo di carattere: Times New Roman, 12 pt

35 **Abstract:** Silver nanoparticles (AgNPs) are widely used as antibacterial agent and anticancer
36 drug. However, in many cases the low AgNPs stability limits their massive production and
37 broad applications. The use of niosomes as carrier, to protect and envelop AgNPs, can solve
38 these problems. In this study, AgNPs were functionalized with sodium
39 3-mercapto-1-propanesulfonate (3MPS) to induce high hydrophilic behavior, improving

40 their loading in ~~in Tween 20 and Span 20 niosomes. niosomes. AgNPs were loaded in two~~
41 ~~different niosomes, Tween 20 and Span 20, and investigated.~~ Their entrapment efficiency
42 was evaluated ~~by UV analyses and is around~~ 1-4%. Dimensions were investigated by means
43 of DLS ($\langle 2R_H \rangle = 140 \pm 4$ nm and $\langle 2R_H \rangle = 251 \pm 1$ nm respectively for NioTw20+AgNPs
44 and NioSp20+AgNPs) and ~~the nanosize were. -was confirmed compared with those~~ by AFM
45 and SAXS analyses. Moreover, stability was assessed in water up to 90 days, and both in
46 Bovine Serum (BS) and Human Serum (HS) up to 8 hours. In order to characterize the local
47 structure of niosomes, SAXS measurements have been performed on Tween20 and Span20
48 empty ~~niosomes~~ and loaded with AgNPs. The release profiles of hydrophilic probe calcein
49 ~~and lipophilic probe Nile Red~~ were performed in ~~HHEPESEPESES~~ and in human serum. All
50 these features contribute to ~~deeply define~~ characterize the two systems, NioTw20+AgNPs
51 and NioSp20+AgNPs, suitable and promising in the field of biological applications.

52
53 **Keywords:** niosomes; silver nanoparticles; liposomes; plasmonic materials; drug delivery.
54

55 1. Introduction

56
57 It is well known that the body barrier to external pathogenic attacks is represented by the skin,
58 that prevents microbial invasion [1], so every damage or wound can provide an environment for
59 microbial growth, leading to infection and prolonged wound healing [2,3]. The efficacy of antibiotics
60 is superior to that of other drugs, and antibiotics are thus widely used [4,5]. However, the antibiotic
61 resistance is currently a health emergency so drug-resistant bacterial infections are becoming more
62 common with a consequent increase in public spending [5]. Therefore, new materials for the
63 treatment of wound infections are needed [6,7].

64 Small sizes, nanoparticles have the advantage to be characterized by a larger contact surface
65 with bacteria, able to enhance their penetration and bactericidal effects [Porcaro, F.; Carlini, L.;
66 Ugolini, A.; Visaggio, D.; Visca, P.; Fratoddi, I.; Venditti, I.; Meneghini, C.; Simonelli, L.; Marini, C.
67 Synthesis and structural characterization of silver nanoparticles stabilized with
68 3-mercapto-1-propanesulfonate and 1-thioglucose mixed thiols for antibacterial applications.
69 Materials 2016, 9, 1028.].]. A good candidate is represented by silver nanoparticles (AgNPs) that
70 show antibacterial properties and reduce inflammatory response [Li, Y. et al Inflammatory
71 responses to micro/nano-structured titanium surfaces with silver nanoparticles: In vitro; Journal of
72 Materials Chemistry B Volume 7, Issue 22, 2019, Pages 3546-3559], with no drug resistance in
73 gram-negative bacteria [Sanyasi S et al. Polysaccharide-capped silver Nanoparticles inhibit biofilm
74 formation and eliminate multi-drug-resistant bacteria by disrupting bacterial cytoskeleton with
75 reduced cytotoxicity towards mammalian cells ; Scientific Reports Volume 6, 29 April 2016, 24929].

76 AgNPs are one of the most used metals in nanotechnology, due to their amazing chemical
77 physical features. They have a striking anti-microbial activity. In fact, AgNPs are known to cause
78 oxidative lesion that destroys the bacterial cell wall, due to Ag⁺ ions release, facilitating the entry
79 into the cell and the disruption of crucial metabolic processes and halts cell proliferation.

80 Therefore, AgNPs are widely used in several medical devices, such as in coating of bone
81 prosthesis and chiralurgical stents, in orthodontic materials, in bandages [8-11].

82 Moreover, recently, in the last decade, the research field of AgNPs has moved to the possibility
83 of their use as anticancer drug, due to their inherent cytotoxic effect on cancer cells [12].

84 However, instability of silver nanoparticles limits their industrial application in several cases
85 and most of the methods to prepare Ag-NPs, causing environmental pollution and low production
86 efficiency. To overcome this problem, silver nanoparticles are usually loaded onto carriers like [13].

87 Among various antibacterial agents, silver ions and nanosilver (i.e., Ag nanoparticles (NPs))
88 show impressive antimicrobial activity against a broad spectrum of bacteria by destroying infectious
89 microorganisms, and have an attractive feature of relatively low tendency to cause such bacterial
90 resistance against antibiotics [2,7]. The bactericidal effect of Ag NPs is mainly attributed to their
91 small nanoscale sizes and high surface-to-volume ratios, which allow them to relatively quickly
92 release Ag ions and interact with microbial membranes. Recently, hybrids/composites with Ag NPs
93 dispersed on carriers or supports have attracted much attention due to their enhanced antibacterial
94 activity compared with sole Ag NPs [2]. Furthermore, it is of very significance to seek for the optimal
95 choices of carriers to combine with AgNPs in order to construct ideal antibacterial agents. Various
96 AgNPs-based nanocomposites with different structures and morphologies have been developed up
97 to now, such as amorphous silica matrix dispersed with AgNPs [Das.A. et al.; Confinement induced
98 formation of silver nanoparticles in self-assembled micro-granules Colloids and Surfaces A:
99 Physicochemical and Engineering Aspects Volume 577, 20 September 2019, Pages 185-193], AgNPs
100 core@silica shell [Huang, J. et al. Unveiling the growth mechanism of SiO₂/Ag hybrid nanospheres
101 and using for Surface Enhanced Raman Scattering detection; Applied Surface Science Volume 463, 1
102 January 2019, Pages 115-120], silica-core@silver-shell [17e20], mesoporous silicas loaded with Ag NPs
103 [Mofakham, E.B. et al.; Progesterone Release from PDMS-Modified Silica Xerogels Containing Ag
104 Nanoparticles Silicon Volume 11, Issue 2, 15 April 2019, Pages 703-711;

105 Arun Kumar, K.V. et al; Surface plasmon response of silver nanoparticles doped silica
106 synthesised via sol-gel route; Applied Surface Science Volume 472, 1 April 2019, Pages 40-45],
107 hollow mesoporous silica spheres with Ag NPs in cavity [Lin L. et al; Preparation and antibacterial
108 activities of hollow silica-Ag spheres; Colloids and Surfaces B: Biointerfaces Volume 101, 1 January
109 2013, Pages 97-100

110 Nishanthi, S.T. et al; Nanostructured silver decorated hollow silica and their application in the
111 treatment of microbial contaminated water at room temperature; New Journal of Chemistry Volume
112 43, Issue 23, 2019, Pages 8993-9001], fibers coated with Ag NPs [Bonan R.F. et al; In vitro
113 antimicrobial and anticancer properties of TiO₂ blow-spun nanofibers containing silver
114 nanoparticles; Materials Science and Engineering C Volume 104, November 2019, Article number
115 109876

116 Gao A. et al; Efficient antimicrobial silk composites using synergistic effects of violacein and
117 silver nanoparticles; Materials Science and Engineering C Volume 103, October 2019, Article number
118 109821], etc.

119 Although extensive efforts have been devoted to fabricating a lot of these AgNPs-based
120 nanocomposites involving different carriers' structures, there are still few systematic investigations
121 on the effects of structures on antibacterial performance [14].

122 The use of drug delivery systems (DDS) has been proposed to overcome important issues in
123 active pharmaceutical molecules release, such as unfavorable pharmacokinetics and biodistribution
124 with consequent decrease of side effects. Nanocarriers represent an innovative approach to
125 overcome these issues [I. Venditti; Engineered gold-based nanomaterials: morphologies and
126 functionalities in biomedical applications. A mini review; Bioengineering 2019, 6(2), 53;
127 doi.org/10.3390/bioengineering6020053;]. Moreover, the niosomes systems allow to modulate the
128 silver concentration loading in a range of interest for the biological applications (0,3-5,0 µg/mL) and
129 the modulation of release [16].

130 In this research study AgNPs were synthesized using 3-mercapto-1-sodium propanesulfonate
131 (3MPS) to induce hydrophilic behavior improving niosomal entrapment efficiency and reducing
132 bilayer destabilization. AgNPs were loaded in two different niosomes, Tween 20 and Span 20 loaded
133 with AgNPs, producing two different systems, namely NioTw20+AgNPs and NioSp20+AgNPs. A
134 deep physical chemical characterization was carried out to obtain information on hydrophilic
135 AgNPs and their influence on preparation and characterization of Nio+AgNPs. Moreover, stability

Formattato: Non Evidenziato

Commentato [IV1]: Mi sono tenuta generica perché Yusef
2017 trova conc a cui il sistema funziona con azione
citotossica su cellule tumorali! Quindi in realtà conc in cui il
sistema funziona !
Un dubbio... la nostra conc. È 0,5 mg/mL poi messa il 1 L,
giusto? Ne intrappola il 4%...Quindi siamo nel range 1-5
µg/mL ?!

Commentato [CM2]: Non capiamo perché parli della
diluizione in 1 litro...il nostro 4% è calcolato sulla dose di
carico e in effetti ci verrebbe un e.e. di 20 microg/ml...

136 studies were performed in water, bovine serum and human serum to assess their use in biological
137 compartment. Hydrophilic and lipophilic probe The release profiles of hydrophilic probe calcein
138 were performed/obtained in HEPES/HEPES and in human serum. manca una frase conclusiva tipo:
139 Both systems loaded with AgNPs proved to be able to entrap AgNPs, are stable and maintain the
140 ability to entrap also hydrophilic or lipophilic model molecules so are promising systems for
141 biotechnological applications.

142
143

144 2. Experimental

145 2.1 Materials and Methods

146 Silver nitrate (AgNO₃, 99.5%, Sigma-Aldrich, St. Louis, MO, USA) and sodium borohydride
147 (NaBH₄, 98%, Sigma-Aldrich, St. Louis, MO, USA), were used for the synthesis of the nanoparticles.
148 3-mercaptopropanesulfonic acid sodium salt (C₃H₅S₂O₃Na, 3MPS, Sigma Aldrich, 98%) was used
149 as a capping agent. For all of the solutions, we used deionized water (electrical conductivity less than
150 1 μΩ/cm at room temperature) obtained from a Millipore Milli-Q water purification system.
151 HEPES/HEPES salt (Sodium 2-(4-(2-hydroxyethyl) piperazin-1-yl) ethanesulfonate), Cholesterol,
152 Sephadex G75, Pyrene, DPH (1,6-diphenyl-1,3,5-exatriene), Span 20 (sorbitan monolaurate), Tween
153 20 (polyoxyethylene sorbitan monolaurate), Human/Bovine serum, Calcein and Nile Red were
154 purchased from Sigma-Aldrich (Milan, Italy). All other products and reagents were of analytical
155 grade. All of the reagents were purchased from Sigma Aldrich and were used without further
156 purification.

157

158 2.2 Preparation of AgNPs loaded niosomes

159 The AgNPs-3MPS synthesis consisted in a wet reduction of silver nitrate to metallic silver by
160 means of sodium borohydride in presence of 3MPS [Proposito, P.; Mochi, F.; Ciotta, E.; Casalboni,
161 M.; De Matteis, F.; Venditti, I.; Fontana, L.; Testa, G.; Fratoddi, I. Hydrophilic silver nanoparticles
162 with tunable optical properties: Application for the detection of heavy metals in water. Beilstein
163 journal of nanotechnology 2016, 7, 1654-1661.

164 Venditti, I.; Testa, G.; Sciubba, F.; Carlini, L.; Porcaro, F.; Meneghini, C.; Mobilio, S.; Battocchio,
165 C.; Fratoddi, I. Hydrophilic metal nanoparticles functionalized by 2-Diethylaminoethanethiol: a
166 close look at the metal–ligand interaction and interface chemical structure. The Journal of Physical
167 Chemistry C 2017, 121, 8002-8013.

168 Fratoddi, I.; Benassi, L.; Botti, E.; Vaschieri, C.; Venditti, I.; Bessar, H.; Samir, M.A.; Azzoni, P.;
169 Magnoni, C.; Costanzo, A. Effects of topical methotrexate loaded gold nanoparticle in cutaneous
170 inflammatory mouse model. Nanomedicine: Nanotechnology, Biology and Medicine 2019.]

171 Briefly, a solution of AgNO₃ in deionized water (0.200 g in 10 mL) was added in a flask with
172 3MPS water solution (0.830 g in 10 mL) and the mixture was maintained under stirring in argon
173 atmosphere at room temperature for 10 min. Then NaBH₄ water solution (0.220 g in 10 mL) was
174 finally added dropwise, under vigorous stirring. The reaction mixture was allowed to react for 2 h.
175 The obtained black product was centrifuged with deionized water three times (20 min, 5000 rpm) and
176 then characterized.

177 Several niosomal formulations by Tween 20 or Span 20 were prepared using AgNPs-3 MPS at
178 different concentrations. Only results obtained by selected samples in terms of size, ζ-potential,
179 entrapment efficiency and stability features were reported and discussed.

180 AgNPs-3 MPS were loaded into Span 20 and Tween 20 niosomes, through a protocol already
181 used to internalize chemicals [17]. Niosomes were prepared using thin film hydration method [18].
182 Span 20 or Tween 20 (15 mM) and cholesterol (15 mM) were dissolved in organic solvent mixture
183 (chloroform/methanol 3:1 v/v). The solvent was evaporated using rotary evaporator (VV2000,
184 Heidolph, Schwabach, Germany) to form a thin “film”. The film was hydrated using 5 mL of AgNPs
185 solution, vortexed and sonicated at 60 °C and 18%/16% amplitude for 5 min using ultrasonic
186 microprobe (Vibra-Cell VCX-400, Sonics & Materials, Newtown, CT, USA). The unilamellar

187 vesicular suspension was purified by gel filtration chromatography using Sephadex G75 (glass
188 column of 50 × 1.2 cm) with HEPES/HEPES buffer as the eluent. The purified vesicles were filtrated,
189 by using cellulose filters in order to obtain desired dimensions

190 2.3 Characterizations

191 The AgNPs water solution has been characterized by means of UV-VIS spectra of water
192 suspensions were collected using a Perkin-Elmer Lambda 19 spectrophotometer. The dynamic light
193 scattering (DLS) measurements on the AgNPs colloidal suspensions (0.200 mg/mL) at T = 25.0 ± 0.2°C
194 were performed by the Malvern Zetasizer Nano ZS90 instrument (Malvern,UK), as reported in
195 previous studies [17]. The ζ-potential was calculated from the measured electrophoretic mobility by
196 means of the Smolukovsky equation [19]. UV-vis: λ_{max} (nm) 415; DLS: <2R_h> 5 ± 2 nm; ζ-potential: -35
197 ± 2 mV.

199 Mean size, size distribution, and ζ-potential of empty and AgNPs-loaded niosomes were
200 characterized by using DLS. UV-Visible spectroscopy was employed to evaluate the amount of
201 AgNPs entrapped in niosomal formulations.

202 Bilayer characterization has been carried out on empty Span 20 or Tween20 Niosomes and on
203 AgNPs loaded ones, employing DPH and pyrene (lipophilic probes) that provided different bilayer
204 information (fluidity, microviscosity, and polarity)

205 Span 20/Tween 20 (15 mM), cholesterol (15 mM), and DPH solution (2 × 10⁻⁴ M) were codissolved in
206 chloroform/methanol, which was removed using rotatory evaporator (VV2000, Heidolph,
207 Schwabach, Germany), hydrated with HEPES/HEPES buffer or AgNPs solution (0,5 mg/ml), with the
208 same preparation methods above mentioned. Cellulose filter of 450 nm cut off was used to purify the
209 DPH-niosomal formulations. Fluorescent measurements were performed (λ = 350–425 nm) using
210 luminescence spectrometer (LS5013, PerkinElmer) in order to obtain Florescence Anisotropy. The
211 florescence anisotropy (r) was determined by using Equation (1) [20-22].

$$212 \quad 213 \quad A = \frac{I_{vv} - I_{vh} \ x \ G}{I_{vv} + 2I_{vh} \ x \ G} \quad (1)$$

214 where I_{vv}, I_{vh}, I_{hv} and I_{hh} are fluorescent intensities, and subscript V (vertical) and H
215 (horizontal) represent the orientation of polarized light. G factor is ratio of sensitivity of detection
216 system for vertically and horizontally polarized light.

217
218 Pyrene loaded niosomes were prepared by adding the probe (4 mM) to niosomes (Nio)
219 components in order to obtain empty and Nio-AgNPs following the same preparation method as
220 above. Pyrene is a florescence probe, whose monomer exhibited a spectrum characterized with five
221 emission peaks (from I1 to I5) and excimer has only one peak (IE). The monomer and the excimer
222 have different florescence signals, and the ratio between the several florescence intensities is
223 directly related to the probe distribution in the bilayer. In particular, the ratio I1/I3, corresponding to
224 the first and third vibration bands in the pyrene spectrum, is related to the polarity of the probe
225 environment. Pyrene can form intramolecular excimer based on the viscosity of the probe
226 microenvironment [23], and it is estimated with the ratio IE/I3, where IE is the excimer intensity. The
227 florescence signals emitted by pyrene loaded niosome suspension was scanned (λ = 350–550 nm)
228 using luminescence spectrometer (LS5013, PerkinElmer) and intensities of excimer florescence (IE),
229 first (I1), and third (I3) peak were recorded [24].

230 Atomic force microscopy (AFM) study of the morphology of the niosomes has been performed using
231 a standard AFM setup (Dimension Icon, Bruker Inc.) equipped with Si cantilevers suitable for
232 tapping mode imaging. Samples have been prepared by depositing a droplet of solution on a clean
233 monocrystalline Si surface and waiting until partial dehydration. AFM imaging has been performed
234 in air and at room conditions.

235 SAXS experiments were performed at ID02 high-brilliance beamline at the ESRF (Grenoble, France).
236 The measured SAXS profiles report the scattered radiation intensity as a function of the momentum
237 transfer, q = (4π/λ)sin(θ/2), where θ is the scattering angle and λ the x-ray wavelength (0.1 nm).
238

Commentato [S3]: iole:

bisogna uniformare va bene se li chiamiamo sempre
Nio-AgNPs
come in riga 129?

Commentato [CM4]: ok

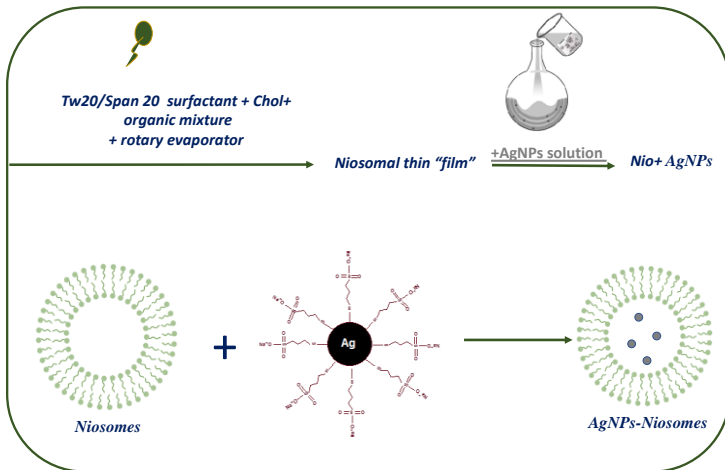
239 Analysis was carried out to obtain information on dimension, homogeneity, shape of the particles in
240 solution. The form factors of niosomes have been reconstructed as uni-lamellar or multi-lamellar
241 closed bilayers. Details are reported in the Supporting information.
242 Biological studies were also carried out in the presence of Bovine or Human serum to evaluate the in
243 vitro stability. Mixtures of empty and AgNPs loaded Nio and 45% of Bovine or Human serum, were
244 prepared and incubated at 37 °C. Analyses were performed at different time intervals (0, 0.5, 1, 2,
245 and 3 h) by DLS (to evaluate variations of particle size and ζ -potential [25].
246 Stability studies up to 90 days at different temperatures, room temperature (RT) and 4°C, were
247 carried out by DLS, to assess dimension and ζ -potential of empty niosomes and Nio -AgNPs [25].
248 Release studies were carried out following the release calcein from empty niosomes and Nio
249 -AgNPs using Fluorimetric apparatus.
250 The hydrophilic probe (calcein 10⁻²M) was added to formulation during film hydration and the
251 excess of calcein was purified with the same technique above mentioned [25].
252 In vitro release experiments were performed at 37°C, defined volume of vesicle dispersions was
253 included in dialysis sacs (cut-off 8.000) with a fixed diffusing area (5.5 cm²) adding to niosomal
254 formulation 45% of human serum or HEPES (in order to maintain the same probe
255 concentration). The probe concentration was detected in the outer solution at fixed time intervals (0,
256 1, 2, 3, 4, 5, 6, 7, 8 and 24 h) by means of the Fluorometric apparatus taking into account the dilution
257 factor.

258 Results and discussion

259 AgNPs were functionalized by 3MPS to induce high hydrophilicity and to control the shape
260 and dimension in the range of 2-5 nm, as already report [F. Mochi, L. Burratti, I. Fratoddi, I. Venditti,
261 C. Battocchio, L. Carlini, G. Iucci, M. Casalboni, F. De Matteis, S. Casciardi, S. Nappini, I. Pis, P.
262 Proposito; Interaction of colloidal silver nanoparticles with Co²⁺ and Ni²⁺ in water for sensing
263 application; Nanomaterials 8 (2018) 488; doi:10.3390/nano8070488www
264 Corsi, P.; Venditti, I.; Battocchio, C.; Meneghini, C.; Bruni, F.; Proposito, P.; Mochi, F.; Capone,
265 B. Designing an Optimal Ion Adsorber at the Nanoscale: The Unusual Nucleation of AgNP/Co²⁺-
266 Ni²⁺ Binary Mixtures. The Journal of Physical Chemistry C 2019, 123, 3855-3860]. In fact, the
267 hydrophilicity is a crucial feature to obtain the insertion in the aqueous core of the niosomes. Even
268 the small dimensions are a key parameter to ensure the inclusion and above all the stability of the
269 final hybrid system, as also reported in the literature [Yusuf 2017]. The AgNPs were loaded into
270 niosomes by adding nanoparticles during the typical preparation protocol of niosomes, as
271 schematized in Figure 1.
272

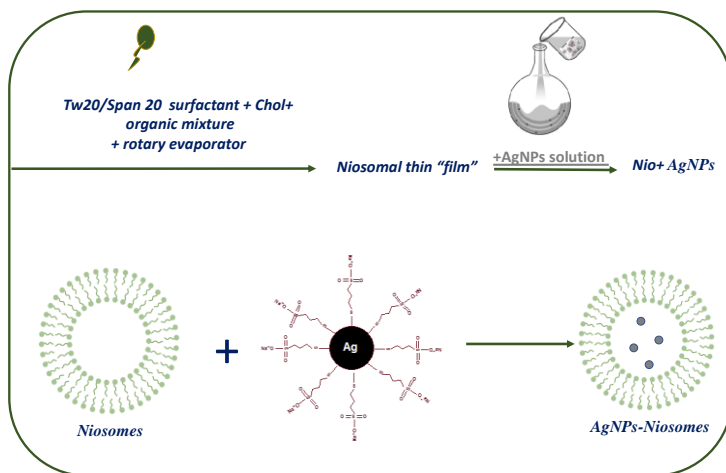
273

274



295

296
297
298
299
300
301
302
303
304
305



306
307
308
309
310

Figure 1 Preparation scheme of Nio – AgNPs preparation.

Commentato [UdMO5]: Va fatta didascalia, se va bene l'immagine...

According to characterization results obtained, the best samples selected were Tween 20/Span 20 niosomes hydrated with AgNPs at the 0,5 mg/ml concentration.

311 The first comparison between empty niosomes and Nio-AgNPs was done by analyzing
 312 hydrodynamic diameter, ζ -potential and PDI (Polydispersity index) by DLS. Results are shown in
 313 table 1.

314 In both niosomal formulations, by Tween 20 or Span 20, all the parameters analysed by DLS are
 315 preserved after the addition of AgNPs. The empty samples show differences in dimensions, due to
 316 the different internal structures determined by the different surfactant employed for niosomal
 317 preparation. In particular Span 20 niosomes, as expected [26] are bigger than Tween 20 ones and
 318 show more negative ζ -potential.
 319
 320

Sample	Hydrodynamic diameter (nm) \pm SD	ζ -potential (mV) \pm SD	PDI \pm SD
NioTw20	136.1 \pm 2.0	-32.8 \pm 0.3	0.38 \pm 0.01
NioTw20+AgNPs	140.3 \pm 3.9	-33.1 \pm 1.4	0.40 \pm 0.01
NioSp20	230.2 \pm 5.9	-42.7 \pm 2.3	0.35 \pm 0.01
NioSp20+AgNPs	251.7 \pm 6.0	-42.9 \pm 1.2	0.40 \pm 0.01

321 Table 1. Hydrodynamic diameter, ζ -potential and PDI of different niosomal formulations.

322
 323 The entrapment efficiency of AgNPs in vesicular systems, was evaluated by means of the
 324 calibration curve (see SI-Fig.2) and results are reported in Table 2.
 325
 326
 327
 328

Samples ID	Entrapment efficiency (mg/mL)
NioTw20 + AgNPs	<1 %
NioSp20 + AgNPs	4 %

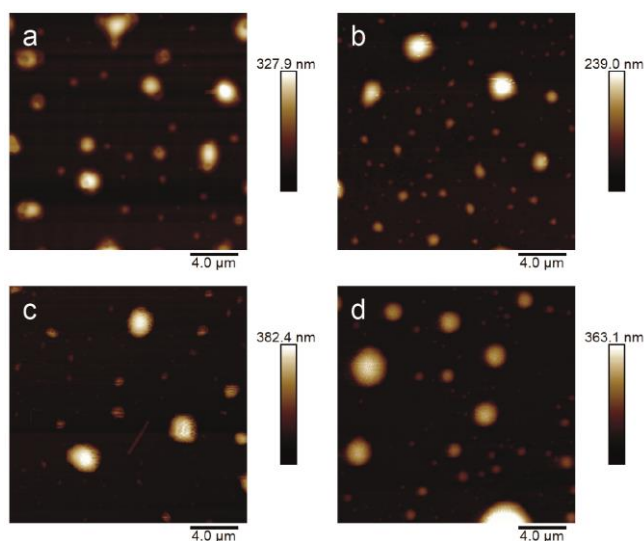
329 Table 2. The trapping efficiency of AgNPs in niosomes

330
 331 The data obtained indicate that entrapment efficiency for the two systems is not the same; better
 332 for Span 20 than Tw20 niosomes, probably related to different internal structure and or capacity
 333 (aqueous volume available to host AgNPs). Moreover, these values allow to assemble systems with a
 334 silver concentration in the range of interest for biological applications (0,3-5,0 μ g/mL) as reported in
 335 literature [16]. Results obtained by bilayer characterization studies (table 3), show no variation in the
 336 evaluated bilayer properties (table 3), thus demonstrating that no interactions occur between
 337 niosomal double layer and AgNPs, that probably will be located inside aqueous compartments.
 338
 339
 340

Sample	Fluidity (Anisotropy)	Microviscosity (I_H/I_S)	Polarity (I_L/I_S)
NioTw20	0.10	0.90	0.90
NioTw20+AgNPs	0.11	0.90	0.90
NioSp20	0.10	1.01	0.94
NioSp20+AgNPs	0.11	1.03	0.90

341 Table 3: Bilayer Characterization Results of Nio and Nio-AgNPs
 342
 343
 344

345 **Morphological studies were performed on empty niosomes and Nio-AgNPs**. Representative
 346 AFM images of the samples are shown in Fig. 2. The morphological characterization indicates that
 347 niosomes have regular spherical shape. Probably due to the intrinsic limitations related to sample
 348 preparation, the size of niosomes seems highly dispersed, according to PDI values by DLS analyses,
 349 the bigger particles being probably the results of agglomeration of individual niosomes.
 350



351
 352
 353 Figure 2: AFM images related to: NioTw20 (Fig. 2 a), NioTw20+AgNPs (Fig. 2 b), NioSp20 (Fig. 2 c)
 354 and NioSp20+AgNPs (Fig. 2 d).
 355

356 In deposited sample, large amorphous particles are visible, likely resulting from coalescence of
 357 several vesicles on the substrate surface as well as the possible partial dehydration make the vesicles
 358 lose their original spherical shape. By a visual inspection, Tween-based niosomes, i.e., NioTw20 (Fig
 359 2a) and NioTw20+AgNPs (Fig. 2 b), are smaller than the Span-based ones, i.e., NioSp20 (Fig. 2 c) and
 360 NioSp20+AgNPs (Fig. 2 d), in qualitative agreement with the measured hydrodynamic diameter
 361 reported in Table 1. Conversely, the effect on the size of the presence of AgNPs cannot be appreciated
 362 in both the Tween and Span based formulation, as expected considering the relatively small
 363 variations evaluated by DLS and the dispersion of the size in AFM samples.

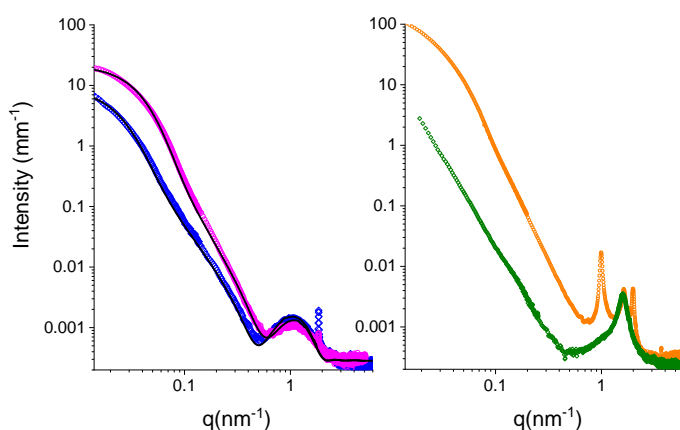
364 In order to characterize the local structure of niosomes, SAXS measurements ~~have been~~ were
 365 performed on Tween20 and Span20 niosomes empty and loaded with AgNPs.

366 In Figure 3 the intensity spectra are reported for Tween20 based nanoparticles (panel A) and for
 367 Span20 based nanoparticles (panel B) in a wide q range ($0.014 \text{ nm}^{-1} \leq q \leq 6 \text{ nm}^{-1}$), corresponding to
 368 distances from 150 nm to the nm. Differences in the intensity profiles are clearly visible for the two
 369 systems in all regions of the spectra. Besides the feature of the form factor of the particles in solution
 370 a small diffraction peak at 1.84 nm^{-1} , corresponding to a characteristic distance of 3.41 nm, is well
 371 known, and stems for the presence of cholesterol crystallites in surfactants/cholesterol mixtures [27].

Commentato [S6]: mi sembra che usiamo sempre passato

Formattato: Non Barrato

372 Crystallites could be either excluded from the bilayers, in peripheral contact, for example, or
 373 included in the bilayers, as segregated structures.
 374



375
 376
 377 Figure 3 SAXS spectra of Tween 20 and Span 20 based niosomes. Panel A. Tween 20 based empty
 378 niosomes (blue diamonds) and AgNPs-Nio-AgNPs (magenta dots). Fitting curves have been
 379 obtained by modelling the particle as an internal solvent core surrounded by a surfactant closed
 380 bilayer (for details see Supporting Information.....). Panel B. Span 20 based empty niosomes (green
 381 diamonds) and AgNPs-Nio-AgNPs (orange dots).
 382

383 Tween20 based particles display a niosomes shape, characterized by a local bilayer structure
 384 with thickness of about 6 nm, being the hydrophobic core of 2.5 nm and the two hydrophilic layers
 385 of 1.6 nm and of 2 nm, respectively. Moreover, the absence of peaks due to multilamellar
 386 organization, reveals that the adopted structure is unilamellar.

387 In the presence of AgNPs Tween 20 niosomes keep a local unilamellar structure, with unaffected
 388 structural features. On the other hand, in the low-q region of the spectrum, the scattered intensity
 389 increases by one order of magnitude. The form factor of the unilamellar closed particles can be
 390 modelled replacing the internal water with a higher electron density solvent, confirming the
 391 presence of AgNPs entrapped inside the aqueous core of the niosomes.

392 Span 20 based aggregates display the characteristic features of closed lamellar-type particles.
 393 Nevertheless, the local structure of Span 20 based niosomes is quite different from the Tween 20
 394 based one. A broad intensity peak is clearly visible at $q = 1.6 \text{ nm}^{-1}$, together with a very broad left
 395 shoulder. The position of the peak corresponds to a characteristic distance $d = 3.9 \text{ nm}$, compatible
 396 with twice the length of a Span 20 (sorbitan monolaurate) molecule. Results indicate that Span 20
 397 niosomes are multilamellar closed particles, with a water core surrounded by a peculiar layered
 398 shell: several adjacent concentric bilayers are in close contact, heads to heads, without any water
 399 penetration. The scattered intensity profile of Span20-based loaded niosomes, reported in Figure 3
 400 (panel B), presents a pronounced increase in the low-q region, sign of the presence of AgNps
 401 enclosed in the internal aqueous core of the niosomes. The increase is definitely higher than the one

Commentato [UdMO7]: Vi mandiamo in allegato supporting information di elena...se serve

Commentato [UdMO8]: Una volta deciso l'ordine va messo il numero della figura

observed in Tween 20 based AgNPs-Nio-AgNPs , suggesting that Span 20 is more efficient in entrapping metallic NPs. On the local scale, two additional peaks at $q = 1 \text{ nm}^{-1}$ and $q = 2 \text{ nm}^{-1}$ are visible, revealing a swollen multilamellar structure with characteristic distance $d = 6 \text{ nm}$, coexisting with the tight one at $d = 3.9 \text{ nm}$. The 6 nm distance is typical for lipid multilamellar structures and also found in Tween $\text{\textcircled{R}}$ 20-derivatives/cholesterol niosomes [27]. The presence of AgNPs induces partial disjunction of adjacent bilayers with an increased water penetration.

Stability studies of NioTw20/NioTw20+AgNPs and NioSp20/NioSp20+AgNPs were performed in bovine serum and human serum to compare their behavior in biological compartment, as shown in Figure 4. Empty niosomes are stable both at room temperature and at 4°C , while Nio-AgNPs showed a different behavior in terms of dimensional increase at RT conditions, not confirmed at 4°C storage temperature. Colloidal stability at 4°C is higher because of reduced collision events of the dispersed particles and hence coalescent phenomena.

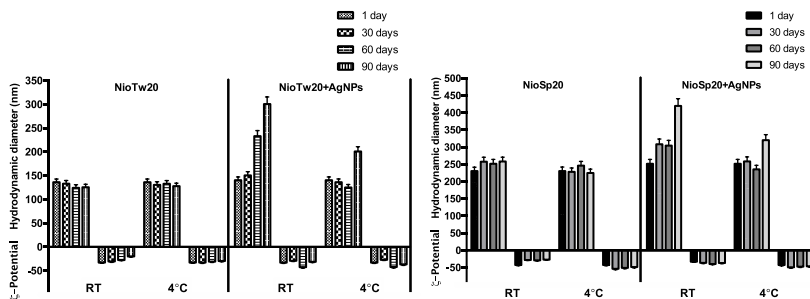
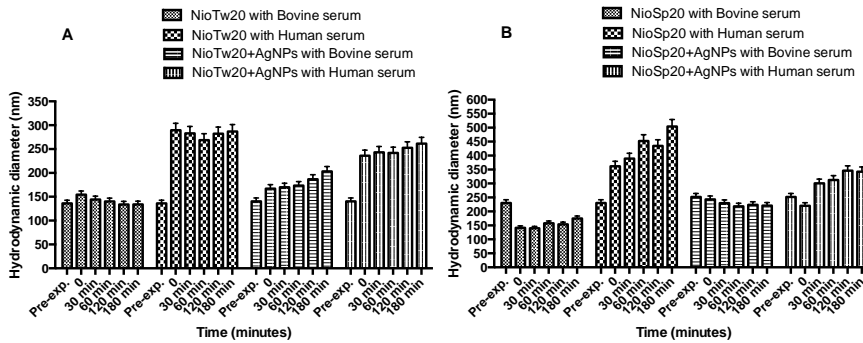


Figure 4. Stability studies of empty niosomes and Nio-AgNPs at room temperature and 4°C .

The effect of the serum (human and bovine) is another important element to evaluate in order to define the interaction between vesicles and fluids. Experiments were performed at 37°C evaluating the size and ζ -potential (data not shown) variations by DLS analysis up to 3h (Figure 5). During the time interval analyzed, the same trend is observed for all vesicles. Vesicles in 45% bovine serum do not show a dimensional increase, while in 45% human serum the trend is different. The different protein composition of human serum is the reason of the attractive interaction between negatively charged niosomal surface and proteins. These interactions are strong enough to observe the same populations for the three hours.



428

429

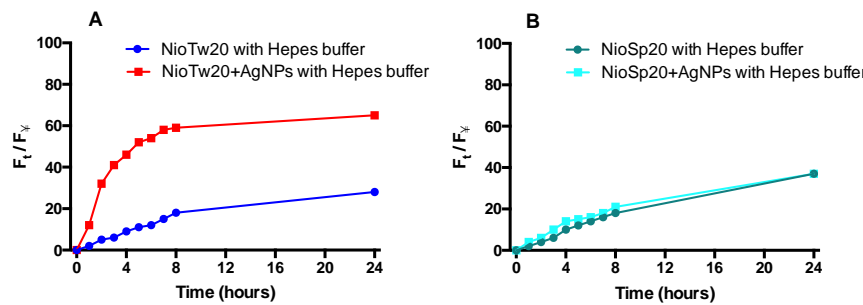
430 Figure 5: Niosomal biological stability at 37°C in different media. A) NioTw20/AgNPs in bovine and
 431 human serum; B) NioSp20/AgNPs in bovine and human serum.

432

433 In order to confirm the ability of Nio to release lipophilic and hydrophilic probes, also in
 434 presence of AgNPs, calcein and Nile Red release studies were carried out. Qui andrebbe messa frase
 435 che spiega perché è stato fatto questo esperimento con calceina, tanto per rendere più fluido il
 436 discorso.

437 In figures 6 and 7 release profiles of the hydrophilic probe calcein and Nile Red are reported
 438 che temperature questo esperimento. In each experiment, the calcein release data from empty
 439 niosomes and NioTw20 AgNPs were compared in order to evaluate the influence of the silver
 440 nanoparticles, entrapped in the same compartment, on the hydrophilic probe release. The calcein
 441 entrapment in both samples was comparable. Experiments were carried out at 37°C both in
 442 HEPES and human serum. The results obtained in human serum are not reported because the
 443 calcein release was not significant (20%) probably due to coating and masking effects of serum,
 444 which makes it difficult to quantify the calcein release in the external medium. In HEPES
 445 buffer, the presence of AgNPs influences the release profile of calcein only in NioTw20 formulation.
 446 As demonstrated by SAXS analyses, only a double layer is present, so more susceptible to silver
 447 nanoparticles destabilization. Calcein release by this sample is around 65% in 24 hours, respect to
 448 30% by NioSp20/AgNPs, where the presence of different bilayer can make more difficult calcein
 449 release.

450



451

452

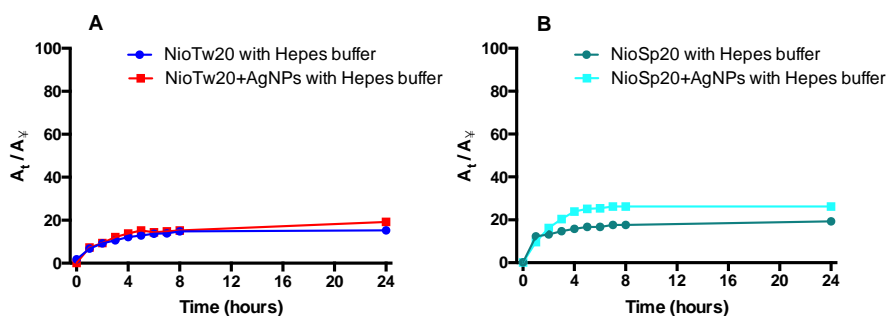
453 Figure 6: Calcein release studies in HEPES buffer at 37°C temperature from: A)
 454 NioTw20/AgNPs calcein release profiles in HEPES buffer; B) NioSp20/AgNPs calcein release
 455 profiles in HEPES buffer.

456
457
458
459
460
461
462
463
464
465

On the contrary, in both samples Nile Red release profiles, obtained in HEPES/HEPES at 37°C, are comparable, because of the lipophilic nature of the probe, as shown in figure 7.

Formattato: Non Barrato

The number of bilayers to cross is the limiting step for hydrophilic probe release, while it is not for lipophilic probe, that probe that is located in the bilayer and will be barely released for the poor affinity with the aqueous external medium.



466
467
468
469
470
471
472
473

Figure 7: Nile Red release studies in HEPES/HEPES buffer at temperature 37°C A) NioTw20/AgNPs in HEPES buffer; B) NioSp20/AgNPs in HEPES buffer.

The morphological structure of the two different niosomal formulations and the presence or not AgNPs, could to influence the release profiles of the two probes. Frase finale???

474 **4. Conclusions** potete scrivere voi conclusioni?

This study confirms the possibility of preparing niosomal vesicles by Tween 20, or Span 20 loaded with AgNPs which, as expected, enter are located inside the aqueous compartment of the two systems, as confirmed by the SAXS data, that also allow ; these have allowed to highlight the different structure of the double layer of the studied samples. Our experiments make us think that show that the samples prepared with the surfactant

Span 20 trapped particles more efficiently than Tween 20, reaching the concentration at which metallic nanoparticle effects are observed on in vitro cell cultures, as demonstrated by studies reported in the literature [1635]; in vesicles based on Tween 20 the concentration reached is lower but presumably such as to fall within the efficacy range of the nanoparticles.

Formattato: Non Evidenziato

The systems we study are could be important in increasing skin permeation for biological applications. ; this data, together with the ability to transport silver nanoparticles with antibacterial activity, emerged from the thesis work, makes them an innovative drug delivery system for the treatment of skin lesions and chronic skin diseases.

The studies carried out during my thesis work have revealed a different behavior of the samples prepared on the basis of their surfactant composition, the loading with the silver nanoparticles, and according to the medium in which they were placed.

Formattato: Rientro: Prima riga: 0 cm

In particular, it was found that the formation of the niosomal vesicles also occurs in the presence of the AgNPs, which, as expected, enter the aqueous compartment of the system, as confirmed by the SAXS data; these have allowed to highlight the different structure of the double layer of the studied samples. Our experiments make us think that the samples prepared with the surfactant Span 20 trapped particles more efficiently than Tween 20, reaching the concentration at which metallic nanoparticle effects are observed on in vitro cell cultures, as demonstrated by studies reported in the literature [1635]; in vesicles based on Tween 20 the concentration reached is lower but presumably such as to fall within the efficacy range of the nanoparticles.

497

498 ~~Text to be automatically generated by the MDPI publishing system. Do not delete or modify this text.~~

499 **Supplementary Materials:** The following are available online at www.mdpi.com/xxx/s1, Figure S1:
500 title, Table S1: title, Video S1: title.

501 **Author Contributions:** Conceptualization, C.M., M.C., I.V. and I.F.; Chemical synthesis and
502 characterizations of AgNPs: I.V. and I.F.; Chemical synthesis of niosomes and silver doped niosomes
503 C.M., F.R., M.C.; SAXS investigations: E.d.F., J.M.; AFM investigations: D.P., M.R., L.A.; all authors
504 reviewed and approved the entire manuscript.

505 **Funding:** Please add: “This research received no external funding” or “This research was funded by
506 [name of funder] grant number [xxx]” and “The APC was funded by [XXX]”. Check carefully that
507 the details given are accurate and use the standard spelling of funding agency names at
508 <https://search.crossref.org/funding>, any errors may affect your future funding.

509 **Acknowledgments:** The Grant of Excellence Departments, MIUR (ARTICOLO 1, COMMI 314 - 337
510 LEGGE 232/2016), is gratefully acknowledged by Dr. Iole Venditti.

511 **Conflicts of Interest:** The authors declare no conflict of interest.

512

513 In the text, reference numbers should be placed in square brackets [], and placed before the
514 punctuation; for example [1], [1–3] or [1,3]. For embedded citations in the text with pagination,
515 use both parentheses and brackets to indicate the reference number and page numbers; for
516 example [5] (p. 10), or [6] (pp. 101–105).

517

- 518 1. Author 1, A.B.; Author 2, C.D. Title of the article. *Abbreviated Journal Name* **Year**, *Volume*, page
519 range, DOI.
- 520 2. Author 1, A.; Author 2, B. Title of the chapter. In *Book Title*, 2nd ed.; Editor 1, A., Editor 2, B.,
521 Eds.; Publisher: Publisher Location, Country, 2007; Volume 3, pp. 154–196, ISBN.
- 522 3. Author 1, A.; Author 2, B. *Book Title*, 3rd ed.; Publisher: Publisher Location, Country, 2008; pp.
523 154–196, ISBN.
- 524 4. Author 1, A.B.; Author 2, C. Title of Unpublished Work. *Abbreviated Journal Name stage of*
525 *publication*
526 (under review; accepted; in press).
- 527 5. Author 1, A.B.; Author 2, C.D.; Author 3, E.F. Title of Presentation. In Title of the Collected Work (if
528 available), Proceedings of the Name of the Conference, Location of Conference, Country, Date of
529 Conference; Editor 1, Editor 2, Eds. (if available); Publisher: City, Country, Year (if available); Abstract
530 Number (optional), Pagination (optional).

531

532

533

534

535

536

References

537

- 538 1. Porcaro, F.; Battoecchio, C.; Antocchia, A.; Fratoddi, I.; Venditti, I.; Fracassi, A.; Luisetto, I.; Russo, M.;
539 Polzonetti, G. Synthesis of functionalized gold nanoparticles capped with
540 3-mercaptopropylsulfonate and 1-thioglucoyl mixed thiols and “in vitro” bioresponse. *Colloids and*
541 *Surfaces B: Biointerfaces* **2016**, *142*, 408–416.
- 542 2. Porcaro, F.; Carlini, L.; Ugolini, A.; Visaggio, D.; Visca, P.; Fratoddi, I.; Venditti, I.; Meneghini, C.;
543 Simonelli, L.; Marini, C. Synthesis and structural characterization of silver nanoparticles stabilized
544 with 3-mercaptopropylsulfonate and 1-thioglucoyl mixed thiols for antibacterial applications.
545 *Materials* **2016**, *9*, 1028.

- 546 3. Proposito, P.; Mochi, F.; Ciotta, E.; Casalboni, M.; De Matteis, F.; Venditti, I.; Fontana, L.; Testa, G.;
547 Fratoddi, I. Hydrophilic silver nanoparticles with tunable optical properties: Application for the
548 detection of heavy metals in water. *Beilstein journal of nanotechnology* **2016**, *7*, 1654-1661.
- 549 4. Venditti, I.; Testa, G.; Scubba, F.; Carlini, L.; Porcaro, F.; Meneghini, C.; Mobilio, S.; Battocchio, C.;
550 Fratoddi, I. Hydrophilic metal nanoparticles functionalized by 2-Diethylaminoethanethiol: a close look
551 at the metal–ligand interaction and interface chemical structure. *The Journal of Physical Chemistry C*
552 **2017**, *121*, 8002-8013.
- 553 5. Fratoddi, I.; Benassi, L.; Botti, E.; Vaschieri, C.; Venditti, I.; Bessar, H.; Samir, M.A.; Azzoni, P.;
554 Magnoni, C.; Costanzo, A. Effects of topical methotrexate loaded gold nanoparticle in cutaneous
555 inflammatory mouse model. *Nanomedicine: Nanotechnology, Biology and Medicine* **2019**.
- 556 6. Mochi, F.; Venditti, I.; Fratoddi, I.; Battocchio, C.; Carlini, L.; Iucci, G.; Casalboni, M.; Matteis, F.D.;
557 Casciardi, S.; Proposito, P. Interaction of Colloidal Silver Nanoparticles with Ni²⁺: Sensing
558 Application. In *Proceedings of Multidisciplinary Digital Publishing Institute Proceedings*; p. 427.
- 559 F. Mochi, L. Burratti, I. Fratoddi, I. Venditti*, C. Battocchio, L. Carlini, G. Iucci, M. Casalboni, F. De Matteis, S.
560 Casciardi, S. Nappini, I. Pis, P. Proposito; Interaction of colloidal silver nanoparticles with Co²⁺ and
561 Ni²⁺ in water for sensing application; *Nanomaterials* **8** (2018) 488; doi:10.3390/nano8070488www
- 562 7. Corsi, P.; Venditti, I.; Battocchio, C.; Meneghini, C.; Bruni, F.; Proposito, P.; Mochi, F.; Capone, B.
563 Designing an Optimal Ion Adsorber at the Nanoscale: The Unusual Nucleation of AgNP/Co²⁺–Ni²⁺
564 Binary Mixtures. *The Journal of Physical Chemistry C* **2019**, *123*, 3855-3860.
- 565 8. Blaske, F.; Reifschneider, O.; Gosheger, G.; Wehe, C.A.; Sperling, M.; Karst, U.; Hauschild, G.; Holl, S.
566 Elemental bioimaging of nanosilver-coated prostheses using X-ray fluorescence spectroscopy and
567 laser ablation-inductively coupled plasma-mass spectrometry. *Analytical chemistry* **2013**, *86*, 615-620.
- 568 9. Corrêa, J.M.; Mori, M.; Sanches, H.L.; Cruz, A.D.d.; Poiate, E.; Poiate, I.A.V.P. Silver nanoparticles in
569 dental biomaterials. *International journal of biomaterials* **2015**, 2015.
- 570 10. Knetsch, M.L.; Koole, L.H. New strategies in the development of antimicrobial coatings: the example
571 of increasing usage of silver and silver nanoparticles. *Polymers* **2011**, *3*, 340-366.
- 572 11. Samuel, U.; Guggenbichler, J. Prevention of catheter-related infections: the potential of a new
573 nano-silver impregnated catheter. *International Journal of Antimicrobial Agents* **2004**, *23*, 75-78.
- 574 12. Zhang, X.-F.; Liu, Z.-G.; Shen, W.; Gurunathan, S. Silver nanoparticles: synthesis, characterization,
575 properties, applications, and therapeutic approaches. *International journal of molecular sciences* **2016**, *17*,
576 1534.
- 577 13. Ran, L.; Zou, Y.; Cheng, J.; Lu, F. Silver nanoparticles in situ synthesized by polysaccharides from
578 *Sanguangporus sanguang* and composites with chitosan to prepare scaffolds for the regeneration of
579 infected full-thickness skin defects. *International journal of biological macromolecules* **2019**, *125*, 392-403.
- 580 14. Wang, Y.; Wang, Y.; Su, L.; Luan, Y.; Du, X.; Zhang, X. Effect of surface topology morphologies of silica
581 nanocarriers on the loading of Ag nanoparticles and antibacterial performance. *Journal of Alloys and*
582 *Compounds* **2019**, *783*, 136-144.
- 583 15. Marianecchi, C.; Di Marzio, L.; Rinaldi, F.; Celia, C.; Paolino, D.; Alhaique, F.; Esposito, S.; Carafa, M.
584 Niosomes from 80s to present: the state of the art. *Advances in colloid and interface science* **2014**, *205*,
585 187-206.
- 586 16. Yusuf, A.; Brophy, A.; Gorey, B.; Casey, A. Liposomal encapsulation of silver nanoparticles enhances
587 cytotoxicity and causes induction of reactive oxygen species-independent apoptosis. *Journal of Applied*
588 *Toxicology* **2018**, *38*, 616-627.

- 589 17. Rinaldi, F.; Seguela, L.; Gigli, S.; Hanieh, P.; Del Favero, E.; Cantù, L.; Pesce, M.; Sarnelli, G.;
590 Marianecchi, C.; Esposito, G. inPentosomes: An innovative nose-to-brain pentamidine delivery blunts
591 MPTP parkinsonism in mice. *Journal of Controlled Release* **2019**, *294*, 17-26.
- 592 18. Rinaldi, F.; Hanieh, P.N.; Chan, L.K.N.; Angeloni, L.; Passeri, D.; Rossi, M.; Wang, J.T.-W.; Imbriano,
593 A.; Carafa, M.; Marianecchi, C. Chitosan Glutamate-Coated Niosomes: A Proposal for Nose-to-Brain
594 Delivery. *Pharmaceutics* **2018**, *10*, 38.
- 595 19. Sennato, S.; Bordi, F.; Cametti, C.; Marianecchi, C.; Carafa, M.; Cametti, M. Hybrid niosome
596 complexation in the presence of oppositely charged polyions. *The Journal of Physical Chemistry B* **2008**,
597 *112*, 3720-3727.
- 598 20. Rao, H.S.P.; Desai, A.; Sarkar, I.; Mohapatra, M.; Mishra, A.K. Photophysical behavior of a new
599 cholesterol attached coumarin derivative and fluorescence spectroscopic studies on its interaction with
600 bile salt systems and lipid bilayer membranes. *Physical Chemistry Chemical Physics* **2014**, *16*, 1247-1256.
- 601 21. Lakowicz, J.R. *Principles of fluorescence spectroscopy*; Springer Science & Business Media: 2013.
- 602 22. Lentz, B.R. Membrane "fluidity" as detected by diphenylhexatriene probes. *Chemistry and Physics of*
603 *Lipids* **1989**, *50*, 171-190.
- 604 23. Zachariasse, K.A. Intramolecular excimer formation with diarylalkanes as a microfluidity probe for
605 sodium dodecyl sulphate micelles. *Chemical Physics Letters* **1978**, *57*, 429-432.
- 606 24. Ingallina, C.; Rinaldi, F.; Bogni, A.; Ponti, J.; Passeri, D.; Reggente, M.; Rossi, M.; Kinsner-Ovaskainen,
607 A.; Mehn, D.; Rossi, F. Niosomal approach to brain delivery: Development, characterization and in
608 vitro toxicological studies. *International journal of pharmaceutics* **2016**, *511*, 969-982.
- 609 25. Rinaldi, F.; Hanieh, P.N.; Del Favero, E.; Rondelli, V.; Brocca, P.; Pereira, M.C.; Andreev, O.A.;
610 Reshetnyak, Y.K.; Marianecchi, C.; Carafa, M. Decoration of nanovesicles with pH (low) insertion
611 peptide (pHLIP) for targeted delivery. *Nanoscale research letters* **2018**, *13*, 391.
- 612 26. Carafa, M.; Marianecchi, C.; Rinaldi, F.; Santucci, E.; Tampucci, S.; Monti, D. Span® and Tween® neutral
613 and pH-sensitive vesicles: characterization and in vitro skin permeation. *Journal of liposome research*
614 **2009**, *19*, 332-340.
- 615 27. Marianecchi, C.; Di Marzio, L.; Del Favero, E.; Cantù, L.; Brocca, P.; Rondelli, V.; Rinaldi, F.; Dini, L.;
616 Serra, A.; Decuzzi, P. Niosomes as drug nanovectors: multiscale pH-dependent structural response.
617 *Langmuir* **2016**, *32*, 1241-1249.
- 618



© 2018 by the authors. Submitted for possible open access publication under the terms and conditions of the Creative Commons Attribution (CC BY) license (<http://creativecommons.org/licenses/by/4.0/>).